Tailoring Surface Properties of Cellulose Acetate Membranes by Low-Pressure Plasma Processing

Chun Huang, Ching-Yuan Tsai, Ruey-Shin Juang, Hsiang-Chien Kao

Department of Chemical Engineering and Materials Science, Yuan Ze University, Chung-Li 32003, Taiwan

Received 12 January 2010; accepted 1 April 2010
DOI 10.1002/app.32604
Published online 13 July 2010 in Wiley InterScience (www.interscience.wiley.com).

ABSTRACT: The aim of this study was to tailor the surface properties of cellulose acetate membranes using low-pressure plasma processing. Argon (Ar) plasma and Difluoromethane (CH_2F_2) plasma were used to control the surface wettabilities of cellulose acetate membranes. Optical emission spectroscopy was used to examine the various chemical species of low-pressure plasma processing. In this investigation, the plasma-treated surfaces were analyzed by X-ray photoelectron spectroscopy, while changes in morphology and surface roughness were determined with confocal laser scanning microscopy. Ar plasma activation resulted in hydrophilic surface. CH_2F_2 plasma deposited hydrophobic layer onto the cellulose acetate membrane because of strong fluorination of the top layer. The results reveal low-pressure plasma processing is an effective method to control the surface properties of cellulose acetate membranes. © 2010 Wiley Periodicals, Inc. J Appl Polym Sci 118: 3227–3235, 2010

Key words: membranes; surface modification; cellulose acetate; argon plasma; difluoromethane plasma; wettability

INTRODUCTION

In recent years, there has been increasing utilization of cellulose acetate membrane in the manufacturing field because of its excellent properties including low cost, high hydrophilicity, moderate chlorine resistance, good biocompatibility, and it being an environmentally friendly polymer from a sustainable resource. Cellulose acetate membranes can be used in high-performance asymmetric membranes, such as ultrafiltration (UF) and reverse osmosis (RO) membranes for seawater conversion and clinical hemodialysis. Despite the advantages of cellulose acetate membranes, the use is limited because of their low chemical resistance[1] and rapid flux decline[2–4] than hydrophobic asymmetric membranes. Therefore, ideal high-performance asymmetric membranes would combine the excellent fouling resistance of hydrophilic membranes with the high chemical resistance of hydrophobic membranes, which is best achieved through modifying the hydrophilic membranes to be rendered hydrophobic.

Low-temperature plasma processing has displayed great potential for controlling the surface properties of membranes.[5,6] It is well known that the hydrophilicity/hydrophobicity of membrane surfaces can be significantly improved by low-temperature plasma treatment with reactive gases. Exposure of membrane in a plasma environment could introduce surface crosslinking, functionalization, and in certain cases lead to degradation of the membrane.[7] The main advantage of low-temperature plasma surface modification is its ability to change the surface properties without interfering with the bulk properties.[8] This is the particular significance from the viewpoint of preserving the mechanical and physicochemical properties of the membranes to be modified. However, there are few studies focused on surface modification of cellulose acetate membranes by low-temperature plasma processing.

The aim of the this study is to tailor the surface properties of cellulose acetate membranes by low-pressure plasma processing. The surface features of cellulose acetate membranes were studied by static contact angle measurements and a confocal laser scanning microscopy (CLSM). X-ray photoelectron spectroscopy (XPS) analysis determined the change in the surface chemical composition of untreated and plasma-treated cellulose acetate membranes. Optical emission spectroscopy (OES) was used to examine the various plasma species for plasma surface modification. This work is the first step in exploring the potential of argon plasma activation

Correspondence to: C. Huang (chunhuang@saturn.yzu.edu.tw).

Contract grant sponsor: National Science Council of Republic of China; contract grant numbers: 97-2221-E-155-074, 98-2221-E-155-034, 98-2221-E-155-029.

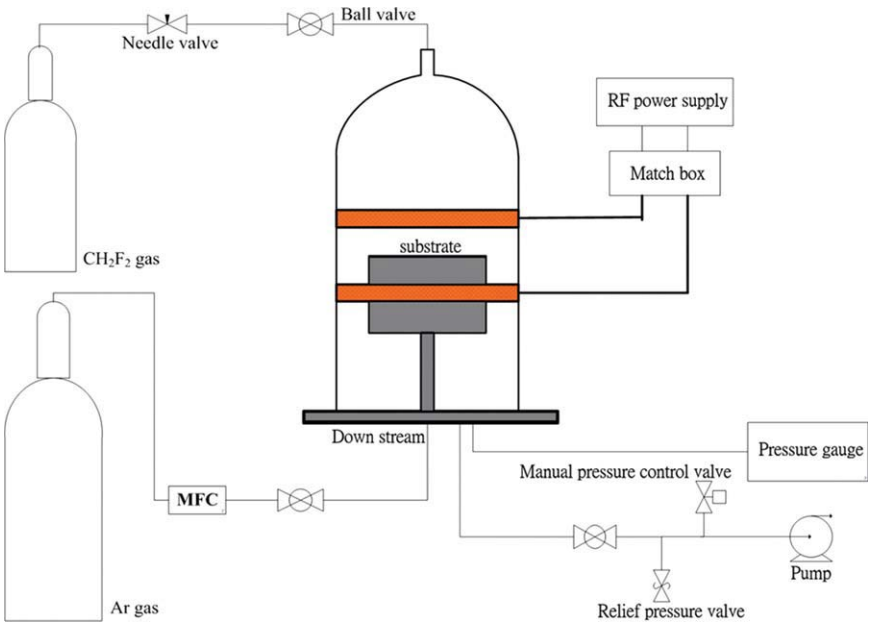

Figure 1 Schematic diagram of the low-pressure plasma system. [Color figure can be viewed in the online issue, which is available at www.interscience.wiley.com.]

and difluoromethane (CH_2F_2) plasma polymerization as a means of controlling the surface of cellulose acetate membranes.

EXPERIMENTAL DETAILS

Argon gas used to create plasma activation was industrial grade with 99.997% purity. Precursor used for plasma polymerization was difluoromethane (CH_2F_2) of 99.97% purity. The plasma reactor system used in this study was a bell jar-type reactor, with dimensions of 44.5 cm in height and 19 cm in diameter, as shown in Figure 1. An electrode assembly with a proprietary design was connected with an RF power source. Argon gas was used as the reactive gas for plasma activation. CH_2F_2 was used as the precursor for plasma deposition. The plasma reactor was first pumped to a base pressure of 1 mTorr or below. Ar/CH_2F_2 was then introduced into the chamber at a preset flow rate and mixing ratio. The system pressure in the reactor was controlled with an MKS pressure controller. When the system pressure reached a preset value, plasma power was

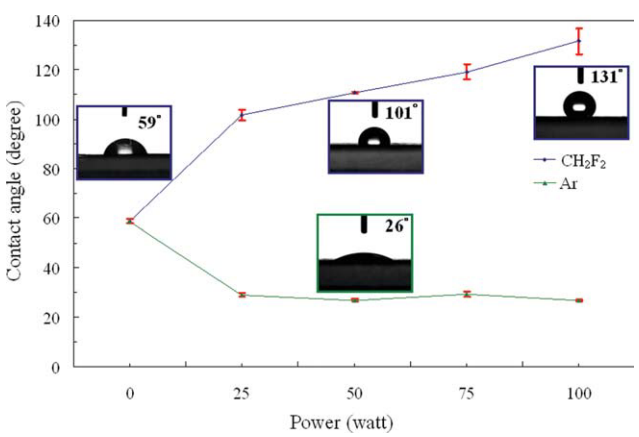

Figure 2 The average contact angle of low-pressure plasma modified cellulose acetate (CA) membrane with different plasma power inputs. Plasma condition: Ar and CH_2F_2 flow rate of 7.5 sccm and 800 mT, at 60 s. [Color figure can be viewed in the online issue, which is available at www.interscience.wiley.com.]

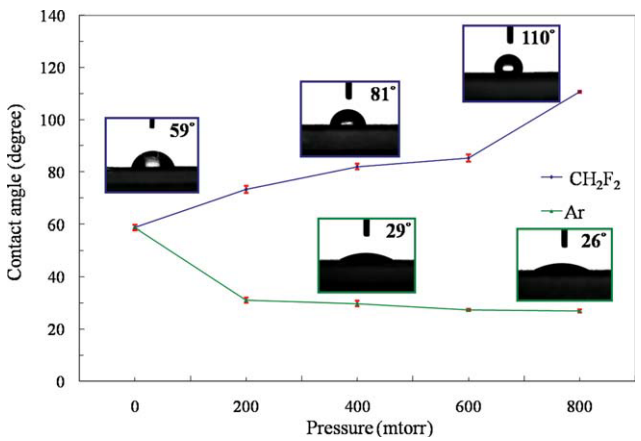

Figure 3 The average contact angle of low-pressure plasma modified cellulose acetate (CA) membrane with different system pressures. Plasma condition: Ar and CH_2F_2 flow rate of 7.5 sccm and RF power 50 Watt, at 60 s. [Color figure can be viewed in the online issue, which is available at www.interscience.wiley.com.]

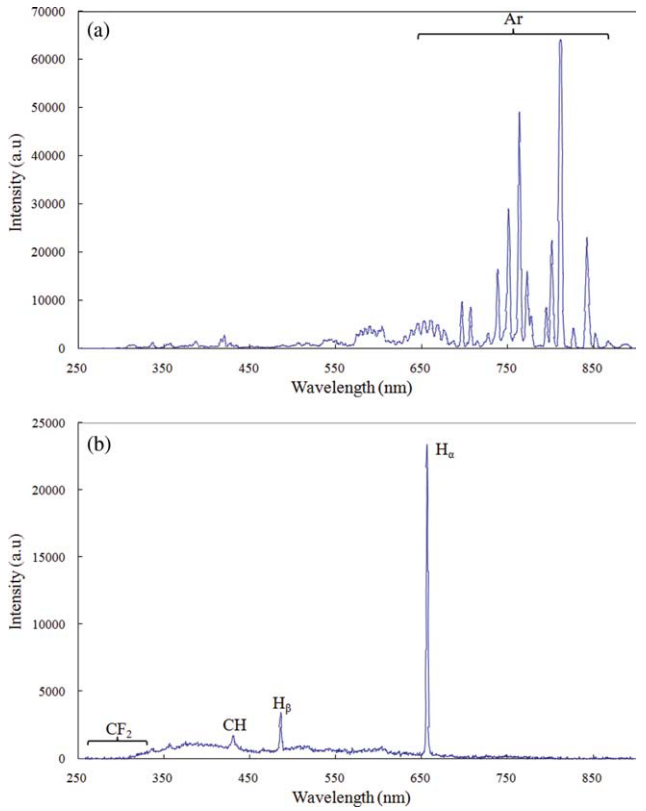

Figure 4 The optical emission spectra from low-pressure (a) Ar plasma and (b) CH_2F_2 plasma. Plasma conditions: RF 50 Watt, 800 mT, 7.5 sccm, at 60 s. [Color figure can be viewed in the online issue, which is available at www.interscience.wiley.com.]

applied at 13.56 MHz with a required match network unit (PFG-300RF generator Huttinger Elektronik, Germany). The static contact angles of plasma-treated cellulose acetate membranes were measured by projecting an image of a sessile droplet resting on a membrane surface with a Magic Droplet Model 100SB Video Contact Angle System (Sindatek Instruments Corporation, Taipei, Taiwan). The surface morphology and roughness of the plasma-treated cellulose acetate membranes were examined by a CLSM. The plasma-treated cellulose acetate membranes were analyzed by a CLSM (VK9700, Keyence Corporation, Japan) with a computer-controlled laser scanning assembly attached to the microscope. The images were processed with VK Viewer control software. The major plasma diagnostic apparatus of Ar/CH_2F_2 plasma is an OES. This equipment consists of both the instrumentation and spectrum analysis software, which was supplied by Hong-Ming Technology. The observable spectral range was 250–950 nm with a resolution of 2 nm FWHM. XPS measurements carried out on a VG Scientific Microlab 310F system, using nonmonochromatic Mg Kα-radiation (hv = 1253.6 eV) and Al Ka-radiation (hv = 1486.6 eV) operated at 25 kV.

RESULTS AND DISCUSSION

Figure 2 shows the dependence of static water contact angles of Ar and CH_2F_2 plasma-treated cellulose acetate membranes with RF plasma power inputs. Water contact angles of Ar and CH_2F_2 plasma-treated cellulose acetate membranes were significantly affected by the RF plasma power input. The average static water contact angles of all CH_2F_2 plasma-treated cellulose acetate membranes increased with increasing RF plasma power input. The increasing plasma power input leads to an increase of the hydrophobicicty. In this case, the number of the hydrophobic polymer-forming-radicals in the plasma grows with an increase of the power. It indicates the polymer-forming-radicals of CH_2F_2 plasma polymerization resulting from the hydrophobic plasma polymerized films on the surface of the cellulose acetate membranes. The static water contact angle values of the Ar plasma-treated cellulose acetate membranes decreased with increasing RF plasma power input. The possible CASING (crosslinking via activated species of inert gases) effect of generating active sites is due to the radicals released from Ar plasma; then, these radicals interact with the cellulose acetate membrane surface to generate dangling bonds which then lead to the formation of the surface active sites.[7] Figure 3 shows the dependence of static water contact angles of Ar and CH_2F_2 plasma-treated cellulose acetate membranes with system pressure. The static water contact angle values of the CH_2F_2 plasma polymerized films for the system pressures of 200, 400, 600, and 800 mT were increased to 73, 81, 85, and 110°. The average static water contact angles of Ar plasma-treated cellulose acetate membranes

TABLE I
Most Intense Emission Lines Observed in Low-Pressure Plasma

Species	Transitions	Energy of emitting state above ground state E_B	Emission wavelength (nm)
CF_2	$A^1B_1 \rightarrow X^1A_1$		250–321
CH	$A^2\Delta$, $v = 0 \rightarrow X^2\Pi$, $v = 0$	<11	431
H_β	$4d^2D \rightarrow 2p^2P^0$	12.7	486
H_α	$3d^2D \rightarrow 2p^2P^0$	12.1	656
Ar	$6s[3/2]^0 \rightarrow 4p[1/2]$	–	639
Ar	$4d[3/2]^0 \rightarrow 4p[1/2]$	–	675
Ar	$4d[3/2]^0 \rightarrow 4p[1/2]$	–	687
Ar	$4p'[1/2] \rightarrow 4s[3/2]$	13.33	697
Ar	$4p'[3/2] \rightarrow 4s'[1/2]^0$	13.48	750
Ar	$4p[3/2] \rightarrow 4s[3/2]^0$	13.17	764
Ar	$4p'[1/2] \rightarrow 4s'[1/2]^0$	–	772
O	$3p^5P \rightarrow 3s^5S^0$	10.74	777
Ar	$4p'[3/2] \rightarrow 4s[1/2]^0$	13.28	795
Ar	$4p[5/2] \rightarrow 4s[3/2]^0$	13.08	812

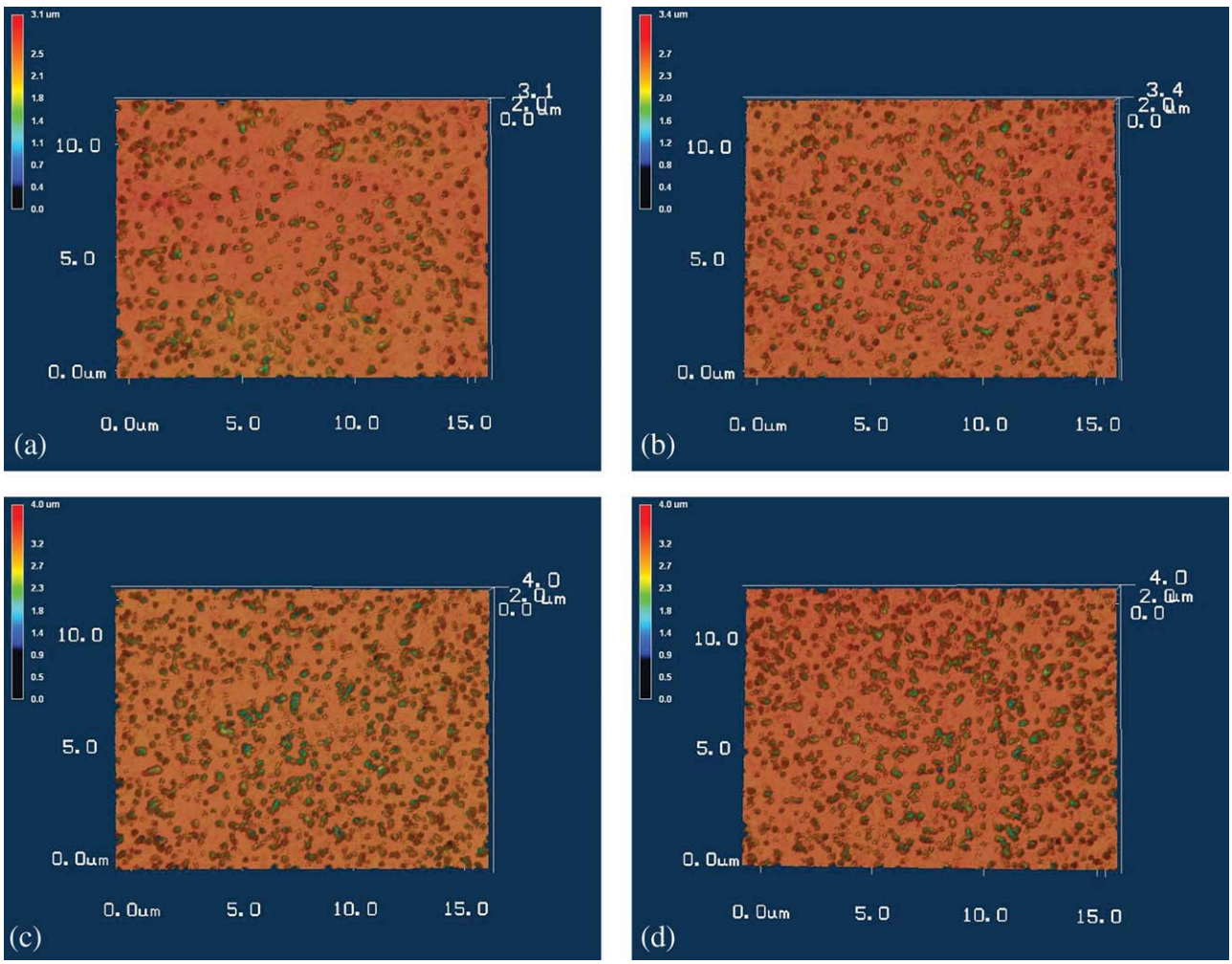

Figure 5 CLSM images of untreated and low-pressure Ar plasma modified cellulose acetate (CA) membrane with different plasma power inputs: (a) untreated, (b) 25 Watt treatment, (c) 50 Watt treatment, and (d) 100 Watt treatment. Plasma condition: Ar flow rate of 7.5 sccm and 800 mT, at 60 s. [Color figure can be viewed in the online issue, which is available at www.interscience.wiley.com.]

decreased to 31, 29, 27, and 26° It also determines at high system gas pressures, the plasma modification efficiency increased because of a lower mean free path of electrons and chemical reaction at higher pressure.

Glow discharge has been mostly been in terms, such as low-pressure plasma, nonequilibrium plasma, glow discharge plasma, and so forth.[9,10] The photo-emitting species are vitally important in luminous gas phase, and the location of glow discharge indicates where the chemically reactive species reaction occurs with the inter-electrode space.[11–14] To distinguish the photo-emitting species, and thus indirectly measure the chemical composition of the glow in the Ar and CH_2F_2 plasma systems, an optical emission spectrometry (OES) was used for diagnosing the plasma. The typical emission spectra of the Ar and CH_2F_2 plasma systems are shown in Figure 4 between 200–900 nm, with few significant emissions outside of this region observed over the 200–1050 nm range of the instrument. Some typical emission lines from the Ar and CH_2F_2 plasma systems are summarized in Table I. Figure 4 shows the feature of optical emission in Ar plasma activation is entirely different from that in CH_2F_2 plasma polymerization. The foremost photoemissions from Ar plasma in Figure 4(a) are the Ar emission lines, which are non-polymerizable. This implies, in plasma surface activation, the chemically reactive species are not only created by electron-impact-dissociation, which occurred at CH_2F_2 plasma polymerization, but also the ionization of argon gas with high energy electrons. From the OES spectra shown in Figure 4(b), the photoemission of CH free radicals that can form plasma polymerization mainly appeared in CH_2F_2 plasma polymerization. The optical emission analysis indicates the possible contribution of hydrophobic plasma polymerized film

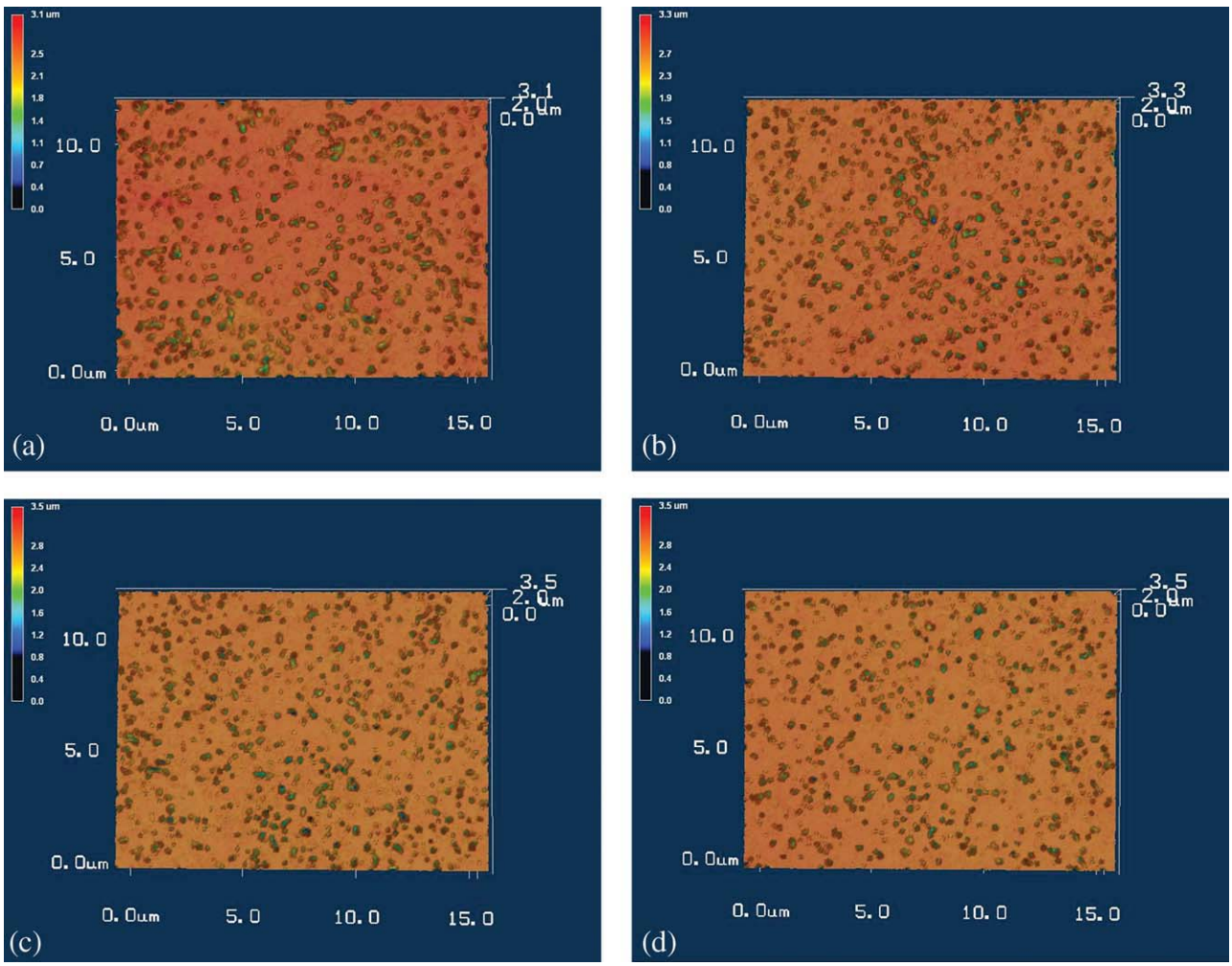

Figure 6 CLSM images of untreated and low-pressure CH_2F_2 plasma modified cellulose acetate (CA) membrane with different plasma power inputs: (a) untreated, (b) 25 Watt treatment, (c) 50 Watt treatment, and (d) 100 Watt treatment. Plasma condition: CH_2F_2 flow rate of 7.5 sccm and 800 mT, at 60 s. [Color figure can be viewed in the online issue, which is available at www.interscience.wiley.com.]

growth mainly occurred at low-pressure plasma polymerization.

Figure 5 shows the CLSM images of the cellulose acetate membrane surfaces obtained in the reflective mode. Many micropores are uniformly distributed on all membrane surfaces. However, it appears the dimensions of most of the pores on the Ar plasma-treated membrane surface are larger than those on the untreated membrane surface. Compared with the unmodified membrane, the pore shapes in the Ar plasma-treated membrane are not regular. This might have been because possible ion bombardment of Ar particles in the plasma state. However, opposite trends can be noted in the images obtained in CH_2F_2 plasma-treated membrane surface (Fig. 6). The dense and regular pore shapes can be observed in CH_2F_2 plasma-treated membrane surface because of the uniform plasma polymerization.

Figures 7 and 8 show the membrane roughness parameters calculated from the three-dimensional CLSM mesh images. The average roughness (Ra) is defined as the average deviation of surface asperities or features from the mean plane; the root mean square roughness (Rq) is the standard deviation of the surface features from the mean plane. The average roughness (Ra) and the root mean square roughness (Rq) values for the modified membrane are 0.188–0.237 μm and 0.341–0.385 μm, respectively. The two values for the unmodified membrane are 0.173 μm and 0.333 μm, respectively. The roughness values for the Ar plasma-treated membrane are more than those of the untreated membrane. The data analysis in Figure 8 also shows the surface area of the CH_2F_2 plasma-treated membrane is smoother than the unmodified membrane in the same projected area. This indicates a uniform plasma polymerized membrane was formed in the CH_2F_2 plasma system.

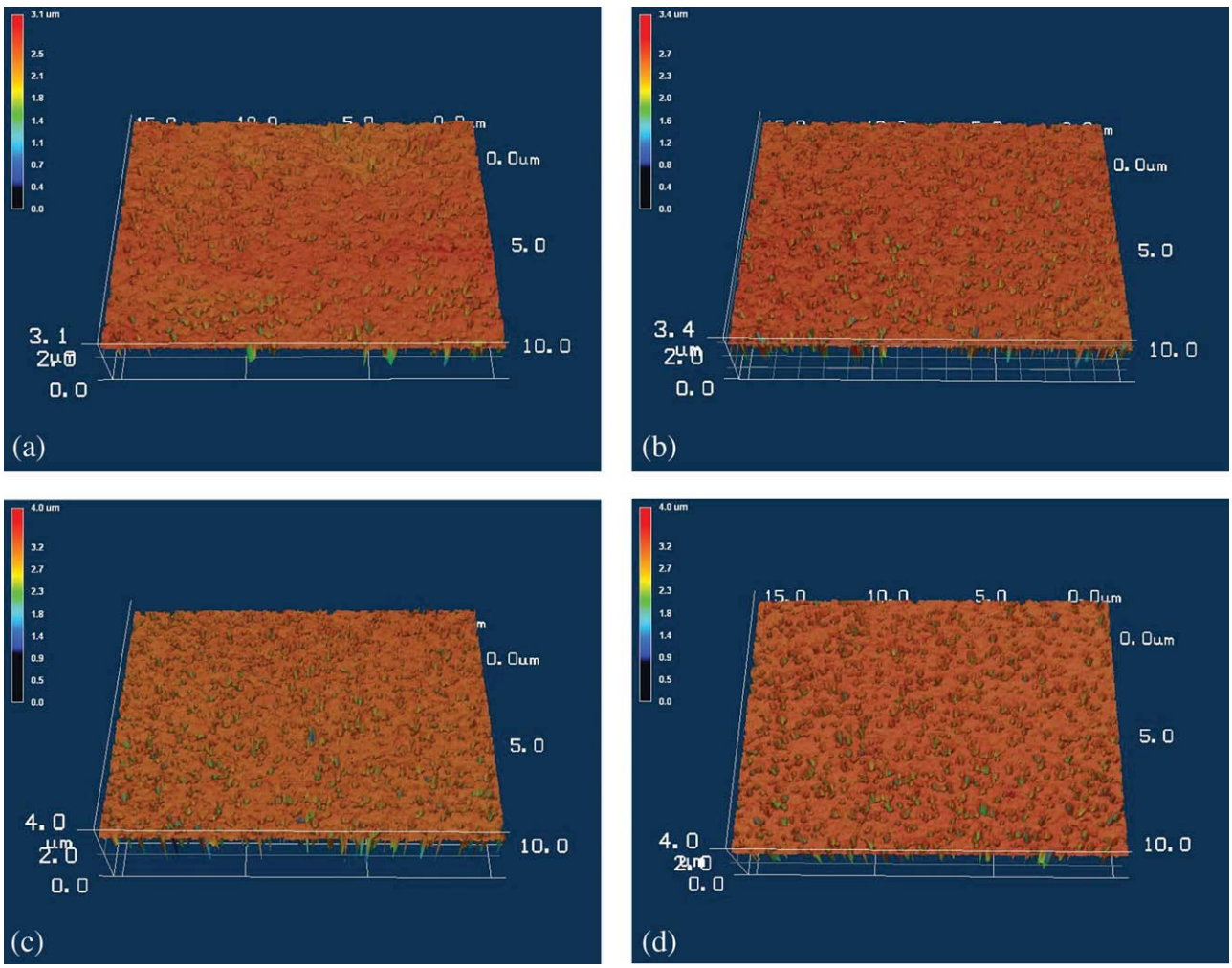

Figure 7 CLSM 3D images of untreated and low-pressure Ar plasma modified cellulose acetate (CA) membrane with different plasma power inputs: (a) untreated, (b) 25 Watt treatment, (c) 50 Watt treatment, and (d) 100 Watt treatment. Plasma condition: Ar flow rate of 7.5 sccm and 800 mT, at 60 s. [Color figure can be viewed in the online issue, which is available at www.interscience.wiley.com.]

The chemical composition of the original cellulose acetate membrane and Ar/CH_2F_2 plasma-treated cellulose acetate membrane surfaces were determined from XPS analysis. The C1s spectra of XPS analysis of the original cellulose acetate membrane and the plasma-treated cellulose acetate membrane are shown in Figure 9. The trend of the intensity change of C1s spectra is correlated with the chemical composition change from XPS analysis in Table II. Figure 9(a) shows the spectrum of untreated cellulose acetate membrane peaks for 284.6 eV and 285.6 eV, corresponding to the C—C and C—O groups, at the same time, additional peaks at 288 eV, and 288.7 eV also appeared because of the O–C—O and O–C=O groups, respectively. The C1s spectrum of Ar plasma-treated cellulose acetate membrane is correlated with the chemical composition change from XPS analysis as shown in Figure 9(b). According to Figure 9(b). the peaks, such as C—O (285.6 eV), O—C—O (288 eV) and O–C=O (288.7 eV) groups arise on the Ar plasma-treated cellulose acetate membrane. The result suggests the oxygen was incorporated with the Ar plasma-treated cellulose acetate membrane surface. The introduction of polar groups onto the cellulose acetate membrane surface may be the main reason for the hydrophilic improvement. C1s XPS-spectrum of CH_2F_2 plasma-treated cellulose acetate membrane was measured and evaluated in Figure 9(c). The spectrum revealed the major contribution of C—CFx (287.5 eV) or CF (289.5 eV) and CF_2^- (292.4 eV) simultaneously. Original peaks at 284.6 eV and 285.6 eV also appeared, implying the chemically reactive fluorocarbon species in CH_2F_2 plasma are mainly deposited on

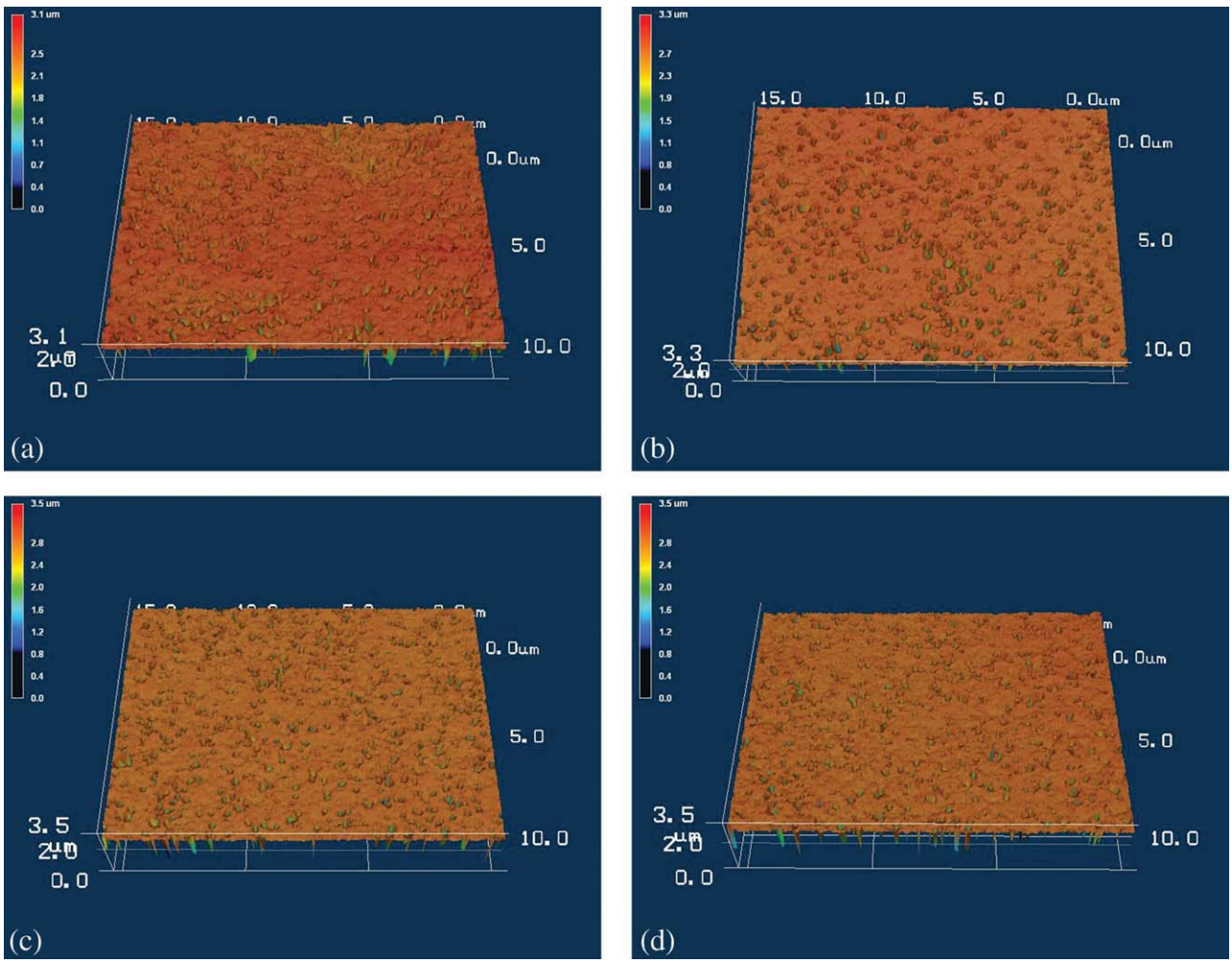

Figure 8 CLSM 3D images of untreated and low-pressure CH_2F_2 plasma modified cellulose acetate (CA) membrane with different plasma power inputs: (a) untreated, (b) 25 Watt treatment, (c) 50 Watt treatment, and (d) 100 Watt treatment. Plasma condition: CH_2F_2 flow rate of 7.5 sccm and 800 mT, at 60 s.

the membrane surface, which obtained low surface free energy to form the hydrophobic surface on the CH_2F_2 plasma-treated cellulose acetate membrane.

The percentage contribution of the C1s components of untreated and low-pressure Ar/CH_2F_2 plasma-treated cellulose acetate membrane, calculated from the C1s core level spectra, is shown in Table II. The concentration of C—C (284.6 eV) decreases while the concentration of oxygen, such as C—O (285.6 eV), O—C—O (288 eV) and O—C=O (288.7 eV) groups increases on the Ar plasma-treated cellulose acetate membrane surface. These polar groups contribute to the increased surface hydrophilicity of the cellulose acetate membrane, suggesting the amount of activated species increases with increasing oxygen content, and the activated species can easily form reactive functional groups on the surface. Table II shows after CH_2F_2 plasma treatment, the C—C(H) groups increased, and additional fluoride deposition groups (C—CFx, CF, and CF_2^-) appeared with respect to CH_2F_2 plasma polymerization.

CONCLUSION

Low-pressure plasma processing was used for controlling the surface properties of cellulose acetate membranes. The objective was to demonstrate the possibility of Ar/CH_2F_2 plasma surface modification. Two approaches were undertaken for controlling the surface properties of the cellulose acetate membranes. One was using Ar plasma for improving surface hydrophilicity and the other was using CH_2F_2 plasma for creating a hydrophobic property. The action of low-pressure plasma processing on cellulose acetate membranes properly controls the surface properties as a result of different mechanisms that decrease or increase the contact angle

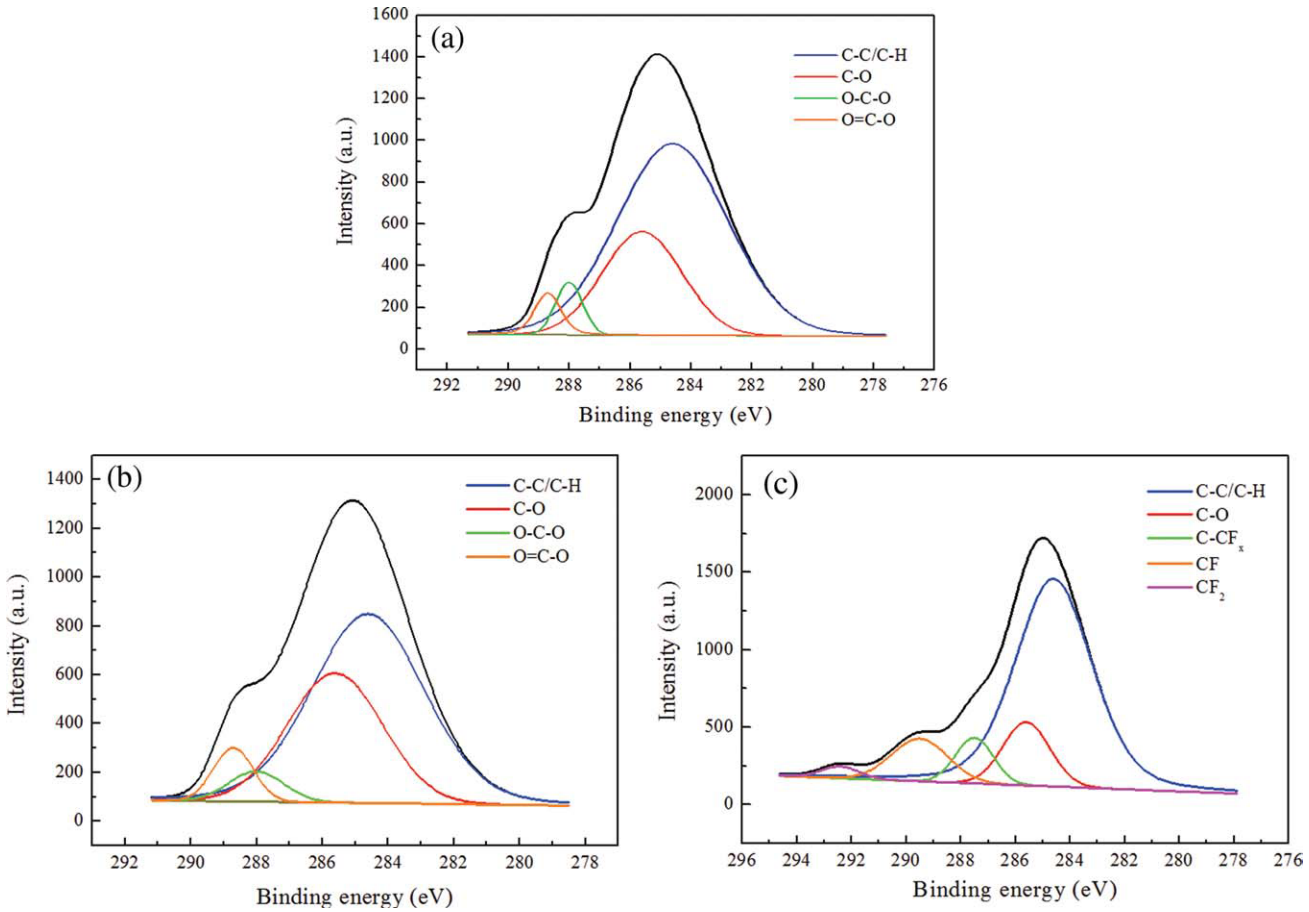

Figure 9 The C1s spectra of XPS analysis of (a) untreated cellulose acetate (CA) membrane and (b) Ar plasma–treated and (c) CH_2F_2 plasma–treated cellulose acetate (CA) membranes. Plasma condition: RF power 50 Watt, Ar and CH_2F_2 flow rate of 7.5 sccm, 800 mT, and treatment time of 1 min. [Color figure can be viewed in the online issue, which is available at www.interscience.wiley.com.]

in the plasma-treated cellulose acetate membranes, mainly by inserting polar groups and in a large fluorine amount increase. The main Ar plasma action is inserting active species in the cellulose acetate membrane surface improves the surface hydrophilicity of the cellulose acetate membranes. The CH_2F_2 plasma polymerization provided excellent hydrophobic properties (greater than 131° of static water contact angle). The possible mechanisms of increased hydrophobicity of the cellulose acetate membranes may be explained by the electron-impact-dissociation in the low-pressure plasma polymerization using optical emission analysis. CLSM micrographs of the plasma-treated cellulose acetate membranes reveal a small change in surface roughness in a qualitative manner. The XPS results show new functional groups on the cellulose acetate membrane surface by Ar/CH_2F_2 plasma. In conclusion, low-pressure plasma processing stands out as very useful method for controlling the surface of cellulose acetate membrane in low-temperature.

TABLE II
The composition/ratio (%) of CIs in the Samples With Different Binding Energy Before and After Plasma Treatment

	Contribution of CIs components (%)						
Sample	C—C/C—H 284.6 eV	C—O 285.6 eV	C—C—O 288 eV	O=C—O 288.7 eV	C—CF_x 287.5 eV	C—F 289.5 eV	C—F_2 292.4 eV
Untreated	65.71	26	4.54	3.75	0	0	0
Ar plasma treated	56.22	33.31	4.57	5.89	0	0	0
CH_2F_2 plasma treated	68.16	12.58	0	0	7.27	10.16	1.84

The authors are thankful for the technique support of R and D Center for Membrane Technology, Chung Yuan University, Chungli, 320, Taiwan.

References

1. Arthanareeswaran, G.; Thanikaivelan, P.; Srinivasn, K.; Mohan, D.; Rajendran, M. Eur Polym J 2004, 40, 2153.
2. Nandi, B. K.; Uppaluri, R.; Purkait, M. K. J Membr Sci 2009, 330, 246.
3. Sen Gupta, B.; Hashim, M. A.; Ramachandran, K. B.; Sen Gupta, I.; Cui, Z. F. Eng Life Sci 2005, 5, 54.
4. Lv, C.; Su, Y.; Wang, Y.; Ma, X.; Sun, Q.; Jiang, Z. J Membr Sci 2007, 294, 68.
5. Matsuyama, H.; Teramoto, M.; Iwai, K. J Membr Sci 1994, 93, 237.
6. Li, K.; Meichsner, J. Surf Coat Technol 1999, 841, 116.
7. Inagaki, N. Plasma Surface Modification and Plasma Polymerization; Technomic Publishing: Lancaster, 1996.
8. Lee, Y. M.; Shim, J. K. Polymer 1997, 38, 1227.
9. Eijkel, J. C. T.; Stoeri, H.; Manz, A. Anal Chem 1999, 72, 2547.
10. Jimenez Zapata, I.; Pohl, P.; Bings, N. H.; Broekaert, J. A. C. Anal Bioanal Chem 2007, 388, 1615.
11. Koufaki, M.; Sifakis, M.; Iliopoulos, E.; Pelekanos, N.; Modreanu, M.; Cimalla, V.; Ecke, G.; Aperathitis, E. Appl Surf Sci 2006, 253, 405.
12. Teixeira, V.; Cui, H. N.; Meng, L. J.; Fortunato, E.; Martins, R. Thin Solid Films 2002, 420, 70.
13. Kregar, Z.; Krstulović, N.; Milošević, S.; Kenda, K.; Cvelbar, U.; Mozetič, M. IEEE Trans Plasma Sci 2008, 36, 1368.
14. Liu, D.; Gu, J.; Feng, Z.; Li, D.; Niu, J. Thin Solid Films 2009, 517, 3011.